Vortex and gap generation in gauge models of graphene

O. Oliveira,[1,2] C. E. Cordeiro,[3] A. Delfino,[3] W. de Paula,[1] and T. Frederico[1]
[1]*Departamento de Física, Instituto Tecnológico de Aeronáutica,12.228-900, São José dos Campos, SP, Brazil*
[2]*Departamento de Física, Universidade de Coimbra, P-3004-516 Coimbra, Portugal*
[3]*Instituto de Física, Universidade Federal Fluminense, 24210-3400- Niterói - RJ, Brazil*
(Received 20 December 2010; revised manuscript received 19 February 2011; published 11 April 2011)

Effective quantum field theoretical continuum models for graphene are investigated. The models include a complex scalar field and a vector gauge field. Different gauge theories are considered and their gap patterns for the scalar, vector, and fermion excitations are investigated. Different gauge groups lead to different relations between the gaps, which can be used to experimentally distinguish the gauge theories. In this class of models the fermionic gap is a dynamic quantity. The finite-energy vortex solutions of the gauge models have the flux of the "magnetic field" quantized, making the Bohm-Aharonov effect active even when external electromagnetic fields are absent. The flux comes proportional to the scalar field angular momentum quantum number. The zero modes of the Dirac equation show that the gauge models considered here are compatible with fractionalization.

DOI: 10.1103/PhysRevB.83.155419 PACS number(s): 71.10.−w, 72.80.Vp, 11.10.Kk

I. INTRODUCTION AND MOTIVATION

In a monolayer of graphene,[1–5] the single-particle dispersion relation near the so-called K and K' Dirac points is linear in $|\vec{k}|$ (see, for example, Refs. 6,7). Formally, it is the dispersion relation of a massless relativistic fermion. Furthermore, the description of the low-energy electronic excitations can be accommodated in a Dirac-type equation. Indeed, starting from a tight-binding Hamiltonian with a hopping parameter independent of the lattice site, one can compute exactly the dispersion relation and expand around the two inequivalent Dirac points to rewrite the dynamical equations of motion for electrons and holes as a Dirac equation in two dimensions with the four-component spinor given by

$$\Psi = \begin{pmatrix} \psi_+^b \\ \psi_+^a \\ \psi_-^a \\ \psi_-^b \end{pmatrix}. \tag{1}$$

The indices a and b refer to the two triangular sublattices, and the $+$ and $-$ indices refer to the two Dirac K and K' points, respectively. For a perfect graphene crystal structure the fermions behave as massless relativistic particles,[8] which translates into the well-known ballistic behavior of the electrons,[9–11] and there is no gap between valence and conduction bands. However, if the two-dimensional honeycomb array of carbon atoms is distorted due to the presence of impurities or to the distortion of the crystal structure, for example, the fermions acquire an effective gap given by half the mass gap. Besides fermion mass generation, the quantum Hall effect,[8,12–17] fractionalization,[18–20] and Berry phases[12] have been observed in two-dimensional graphene-like structures.

Fractionalization in one-dimensional models was investigated more than three decades ago[21–23] within polyacetylene. A similar phenomenon like the fractional quantum Hall effect due to quasiparticle fractional charge and/or fractional statistics can take place in two-dimensional systems.[12,16,17]

A dynamic theory for two-dimensional graphene should describe, of course, its phenomenology and should be able to accommodate for the possibility of gap generation and fractionalization. In Ref. 18 the authors presented a mechanism for electron fractionalization in graphene-like systems keeping time-reversal symmetry. Invoking a Kekulé texture, a complex order parameter Δ_0 was introduced. Δ_0 couples the two Dirac points and changes the electron dispersion relation to $\epsilon(\vec{k}) = (\vec{k}^2 + |\Delta_0|^2)^{1/2}$. Assuming a vortex-like profile $\Delta(\vec{r}) = \Delta(r)e^{in\theta}$, where n is an integer, with $\Delta(r)$ vanishing as $r^{|n|}$ for small r and approaching Δ_0 at large r, fractionalization was associated with the presence of a zero mode of the Dirac kernel. Although fractionalization was connected with the vortex shape of $\Delta(\vec{r})$, in Ref. 18 the authors do not specify the dynamics for the complex vortex profile.

In Ref. 19 a dynamic content to the vortices was introduced through a chiral gauge theory which is compatible with electron fractionalization, extending the work of Hou *et al.*[18] In the language of Ref. 19, vortices are associated with a complex scalar field φ which couples linearly to the fermions. Although a dynamical equation was written [see equations (13) and (14) in Ref. 19], the potential $V(\varphi^*\varphi)$ was left unspecified. From the point of view of quantum field theory (QFT), there is no reason to exclude other types of symmetries and couplings, not present in the model discussed by Jackiw and Pi, without destroying fractionalization.

Indeed, field-theoretical models have been applied to describe nanotubes and graphene physics and have had some success in reproducing their quantum properties (see, e.g., Refs. 24 and 25). In this work, we elaborate on derivative-free fermion-boson and boson self-interactions allowed by QFT principles and discuss possible gauge interactions. The models considered here are a generalization of the results of Ref. 19 and, besides the fermionic field, they consider a complex scalar field φ and a single-gauge vector A_μ field. Moreover, possible ways to distinguish between the different gauge symmetries are discussed.

Our interpretation for the complex scalar field and gauge field is that φ and A_μ resume all the dynamics of the self-interaction of the carbon background and the mean fermionic self-interaction.

The use of scalar and vector potentials to describe some of the graphene properties is not new. Indeed, scalar and vector potentials, including gauge fields, have been used in the literature to describe disorder phenomena, including

distortions of the lattice honeycomb, structural defects, point defects, and self-doping effects associated with the breaking of electron-hole symmetry near the Dirac points, among other properties. A detailed discussion can be found in Refs. 6 and 26 and references therein.

Graphene is an electrically neutral system. On the other hand, graphene has charge carriers. Therefore, it seems natural to associate a charged field with the carbon background. Furthermore, if φ resumes the carbon background self-interactions it should be able to accommodate for the propagation of phonons in the carbon lattice. Phonons feel the density of states of the fermionic degrees of freedom and one expects φ to couple to the density of electron and holes, [i.e., to $\overline{\psi}\psi = -(\psi_+^b)^\dagger\psi_-^a - (\psi_+^a)^\dagger\psi_-^b - (\psi_-^a)^\dagger\psi_+^b - (\psi_-^b)^\dagger\psi_+^a$]. Throughout this paper, we will use the chiral representation for the Dirac matrices, where

$$\gamma^0 = \begin{pmatrix} 0 & -1 \\ -1 & 0 \end{pmatrix}, \quad \vec{\gamma} = \begin{pmatrix} 0 & \vec{\sigma} \\ -\vec{\sigma} & 0 \end{pmatrix}, \tag{2}$$

and

$$\gamma_5 = \begin{pmatrix} 1 & 0 \\ 0 & -1 \end{pmatrix}, \tag{3}$$

where the σ^j stand for the Pauli matrices. Besides the coupling to the density of electron or holes, QFT allows also for a pseudoscalar-like interaction, described by a coupling of φ to $\overline{\psi}\gamma_5\psi = (\psi_+^b)^\dagger\psi_-^a + (\psi_+^a)^\dagger\psi_-^b - (\psi_-^a)^\dagger\psi_+^b - (\psi_-^b)^\dagger\psi_+^a$. The scalar and pseudoscalar interactions couple the two triangular sublattices and the two Dirac points K and K' in different ways. The models discussed in the present work explore contributions coming from both types of interactions (i.e., $\overline{\psi}\psi$ and $\overline{\psi}\gamma_5\psi$).

The potential energy for the complex scalar field φ can accommodate a nonvanishing vacuum expectation value $\langle\varphi\rangle$. If $\langle\varphi\rangle \neq 0$, then the model generates a fermion mass via spontaneous symmetry breaking. On the other hand, if $\langle\varphi\rangle = 0$, the electrons in graphene remain gapless. Therefore, we identify pure graphene with the vacuum state where $\langle\varphi\rangle = 0$, with all other graphene distorted and/or doped states begin described by a different vacuum, and for these $\langle\varphi\rangle \neq 0$.

In what concerns the bosonic fields, the model can accommodate mass gaps both for the scalar and vector excitations. In general, for the gauge theories considered here, a fermion mass gap implies also a vector mass gap. This comes directly from the Higgs mechanism for mass generation. The gap for the scalar excitations is linked with the details of the potential $V(\varphi^\dagger\varphi)$ and is not directly coupled with the fermion and vector gaps. Indeed, we found that the scalar gap can vanish independently of the fermion and vector gaps.

In this paper we also discuss a number of different gauge models which, in principle could be suitable to describe graphene properties. The relation between the spectrum of the scalar and vector excitations with the fermionic spectra depends on which symmetry is gauged. Furthermore, the different connections between fermion, scalar, and vector gaps opens the possibility to check experimentally which of the gauge symmetries, if any, is realized in graphene. Changing the fermion mass gap; for example, by modifying the concentration of impurities and or the distortion of the lattice, and looking at how the scalar or vector mass excitations adjust themselves, one can distinguish between the different gauge models. Besides the pattern of the mass gaps, in general, the models also allow for vortex-like solutions and are compatible with fractional statistics.

These gauge models have finite-energy vortex solutions. For one example, we show that the vortex solution implies the quantization of the "magnetic field" flux. In this case, the Abelian gauge field is connected with the angular momenta of φ along an axis perpendicular to the graphene sheet and, in this sense, the flux of the "magnetic field" is a measure of the angular momenta of φ. This particular solution can be interpreted as consequence of topological defects in the graphene structure and, in principle, phenomena like the Bohm-Aharonov[27–29] effect can occur even when external electric and magnetic fields are absent.

We show that the vortex solutions of nonchiral gauge models presented here have normalizable zero modes of the Dirac equation. The presence of the normalizable zero modes implies fractionalization for graphene, and the quantum Hall effect in graphene sheets could become possible even without chiral gauge symmetry and without external electric and magnetic fields. The observation of the quantum Hall effect in two-dimensional materials without external electromagnetic fields was also discussed within the framework of tight-binding models in the work of Haldane[30] and Hill *et al.*[31] According to the later work, the observation of the quantum Hall effect without an electromagnetic field requires the breaking of the sublattice symmetry, where the two sublattices a and b are interchanged, and the opening of a mass gap at one of the Dirac points, let us say K, while the other Dirac point K' remains gapless. In the class of models discussed here, the mass gap is open, or not, simultaneously at K and K'. Then, according to Ref. 31, the quantum Hall effect without an external magnetic field is not measurable because the contributions from K and K' to the Hall conductivity cancel exactly. The models considered in the present work, although reproducing the tight-binding model in the appropriate limit (see, for example, Ref. 6), give dynamics to all the fields that represent the carbon graphene background and excitations φ and the gauge field. Recall that φ is charged and can give rise to an electric current. In this sense, the models go beyond the tight-binding model, opening the possibility of having a dynamic situation where the conditions explored in Ref. 31 do not apply and, perhaps, may allow the measurement of the quantum Hall effect in graphene. We plan to address this question in a future presentation.

We would like the reader to note that, within the class of gauge models discussed in the present work, fractionalization is allowed without breaking any of the usual discrete symmetries like, for example, time reversal. We do not compute the rich set of zero modes of the Dirac equation but those obtained here are, again, connected with the angular momentum of the complex scalar field φ.

This paper is organized as follows: In Sec. II the effective QFT for graphene is discussed, including its global symmetries. In Sec. III, the different global symmetries are gauged and we discuss how these change the spectra of the scalar, vector, and fermion excitations. Furthermore, combining the information on the different types of gaps, we are able to suggest an experimental test to disentangle which of the gauge

symmetries apply to graphene. In Sec. IV the equations of motion are derived and the vortex solutions for the gauge models are discussed. The short-distance and long-distance properties of the vortex are computed explicitly. The gauge models predict the flux quantization of the "magnetic field" associated with the gauge field. Furthermore, the flux quantization is connected with the angular momenta of φ. In Sec. V the zero-mode solutions of the Dirac equation for a vortex configuration are investigated. Finally, in Sec. VI we resume and conclude.

II. THE EFFECTIVE MODEL

Let us assume that the charge carries (i.e., electrons and holes) are relativistic fermions described by a four-component spinor ψ. The Lagrangian density describing the interaction between fermions ψ and φ can be written as

$$\mathcal{L} = \overline{\psi} i\gamma^\mu \partial_\mu \psi + \partial^\mu \varphi^\dagger \partial_\mu \varphi - P(\varphi)\overline{\psi}\psi - P_5(\varphi)\overline{\psi}\gamma_5\psi - V(\varphi^\dagger\varphi), \tag{4}$$

where the polynomials $P(\varphi)$ and $P_5(\varphi)$ define the type of interaction between fermions and the carbon crystal structure and $V(\varphi^\dagger\varphi)$ defines the self-interactions of the background structure.

The reader should note the linear combination of $P\overline{\psi}\psi$ and $P_5\overline{\psi}\gamma_5\psi$ couplings. Such a freedom would allow to set different couplings to each of the possible fermion chiralities and, in this way, build a chiral theory. Moreover, other Dirac γ matrices are allowed. However, to keep it as simple as possible and to avoid derivative couplings, we will consider in the following only scalar- and pseudoscalar-type interactions.

In a system of units where the action is dimensionless, space and time have dimensions of inverse mass, and for two spatial dimensions and one temporal dimension, ψ has dimensions of mass ($[\psi] \sim M$) and φ has dimensions of the square root of mass ($[\varphi] \sim M^{1/2}$). Requiring that the theory described by $\mathcal{L}$ is perturbatively renormalizable, then for polynomial interactions, naive power counting forbids coupling constants $[g] \sim M^\alpha$ with $\alpha < 0$. This fixes unambiguously the interaction terms to be

$$P(\varphi) = g_1(\varphi + \varphi^\dagger) + g_2\varphi^\dagger\varphi, \tag{5}$$

$$P_5(\varphi) = h_1(\varphi - \varphi^\dagger) + ih_2\varphi^\dagger\varphi, \tag{6}$$

and

$$V(\varphi^\dagger\varphi) = \mu^2(\varphi^\dagger\varphi) + \frac{\lambda_4}{2}(\varphi^\dagger\varphi)^2 + \frac{\lambda_6}{3}(\varphi^\dagger\varphi)^3, \tag{7}$$

up to a constant V_0.

If, in $P(\varphi)$ and $P_5(\varphi)$, one takes $h_1 = -g_1$ and $g_2 = h_2 = 0$, one recovers the Jackiw-Pi theory with their $\varphi^r = 2\mathrm{Re}(\varphi)$ and $\varphi^i = 2\mathrm{Im}(\varphi)$ [see equation (8) in Ref. 19]. In this sense $\mathcal{L}$ generalizes the results of Ref. 19.

Let us discuss now the global symmetries of the model described by the Lagrangiandensity (4).

A. Global $U_A(1)$ symmetry

One of the motivations of Ref. 19 was to build a chiral gauge theory. So let us consider the same type of chiral transformation; that is,

$$\psi \longrightarrow e^{i\omega\gamma_5}\psi, \quad \varphi \longrightarrow e^{i\eta}\varphi. \tag{8}$$

To first order in ω and η, the corresponding variation of the Lagrangian density reads

$$\{2i\omega[h_1(\varphi - \varphi^\dagger) + ih_2(\varphi^\dagger\varphi)] + i\eta g_1(\varphi - \varphi^\dagger)\}\overline{\psi}\psi + \{2i\omega[g_1(\varphi + \varphi^\dagger) + g_2(\varphi^\dagger\varphi)] + i\eta h_1(\varphi + \varphi^\dagger)\}\overline{\psi}\gamma_5\psi. \tag{9}$$

Requiring invariance of $\mathcal{L}$ under the transformation (8), it follows that $g_2 = h_2 = 0$, as in the Jackiw-Pi theory, and $g_1 = \pm h_1$ and $\eta = \pm 2\omega$, with the minus sign recovering the original Jackiw-Pi theory. Note that, from the point of view of (8), invariance of the theory means that the chiral charge associated with φ is, up to a sign, twice the fermionic charge.

The set of transformations (8) with $\eta = \pm 2\omega$ form a group that, from now on, will be called $U_A(1)$. Recall that the Lagrangian density is invariant under $U_A(1)$ if and only if $g_2 = h_2 = 0$ and $g_1 = \pm h_1$.

B. Global $U(1)$ symmetries

Besides the chiral transformation just discussed, the Lagrangian density (4) has further nonchiral $U(1)$ global symmetries. The set of transformations

$$\psi \longrightarrow e^{i\omega}\psi \tag{10}$$

defines the $U_f(1)$ global symmetry of $\mathcal{L}$ and the set

$$\varphi \longrightarrow e^{i\omega}\varphi \tag{11}$$

defines the $U_b(1)$ global symmetry of $\mathcal{L}$ if $g_1 = h_1 = 0$. Furthermore, if $g_1 = h_1 = 0$ in (5) and (6), then the set of transformations

$$\psi \longrightarrow e^{i\omega}\psi, \quad \varphi \longrightarrow e^{i\eta}\varphi, \tag{12}$$

where ω and η are independent parameters, defines another global symmetry of $\mathcal{L}$ called $U_f(1) \otimes U_b(1)$ in what follows. Gauging this symmetry requires the introduction of two gauge fields unless one imposes an additional discrete symmetry with respect to the interchange of the gauge fields. Note that the discrete symmetry gives no constraint on the coupling constants for the fermionic g and bosonic g_φ fields. Indeed, the fermionic covariant derivative reads $D_\mu = \partial_\mu + igA_\mu$, while the bosonic covariant derivative is $D_\mu = \partial_\mu + ig_\varphi A_\mu$, where A_μ is the gauge field. For the sake of simplicity (i.e., to avoid considering more than one gauge field), we will analyze only the $U_f(1) \otimes U_b(1)$ symmetry supplement with the discrete symmetry. Anyway, we will keep using the name $U_f(1) \otimes U_b(1)$ for the symmetry.

C. On the various global symmetries

The various global symmetries are distinguished by the nature of the φ-ψ interaction and by the number of independent coupling constants associated with the gauge field required to define the model.

TABLE I. Global symmetries of the Lagrangian density (4). Recall that, for $U_f(1) \otimes U_b(1)$, we impose an additional discrete symmetry. See text for discussions.

Symmetry	Constraints
$U_A(1)$	$g_2 = h_2 = 0, g_1 = \pm h_1$
$U_f(1)$	none
$U_b(1)$	$g_1 = h_1 = 0$
$U_f(1) \otimes U_b(1)$	$g_1 = h_1 = 0$

The $U_A(1)$ symmetry is not compatible with the interactions $(\varphi^\dagger\varphi)\overline{\psi}\psi$ and $(\varphi^\dagger\varphi)\overline{\psi}\gamma_5\psi$ and only linear-in-φ terms are allowed in the interaction with fermions. Furthermore, the model defines a unique coupling constant.

The $U_f(1)$ symmetry allows linear and quadratic φ couplings to the fermionic field and requires a unique gauge coupling constant.

The local symmetries $U_b(1)$ and $U_f(1) \otimes U_b(1)$ are compatible only with a quadratic φ coupling to the fermion fields. If $U_b(1)$ requires a unique gauge coupling constant, the gauge model with $U_f(1) \otimes U_b(1)$ as a symmetry group includes two independent gauge couplings.

Table I summarizes the global symmetries of Lagrangian density (4) and the corresponding constraints on the φ-ψ coupling constants.

III. GAUGE MODELS AND MASS GAP

The various $U(1)$ symmetries of $\mathcal{L}$ (see Table I), can be made local. Different symmetries will lead to different gauge theories for graphene, after replacing the derivatives by covariant derivatives and adding the corresponding kinetic term for the gauge field. Naturally, the different symmetries will introduce different dynamics which can be seen, for example, at the level of the theory spectra (i.e., at the various mass gaps).

Recall that we are excluding derivative-type couplings. In what concerns the gauge field, not including derivative couplings means that *a priori* we are excluding a Chern-Simons term[32–34]

$$\epsilon^{\alpha\beta\gamma} A_\alpha(\partial_\beta A_\gamma) \tag{13}$$

in $\mathcal{L}$. This type of interaction is allowed by gauge invariance and, in $2+1$ dimensions, is not excluded by the renormalizability requirement.

A. Scalar mass gap

We start our discussion by looking at the scalar excitations in graphene; that is, looking at the mass spectra for the complex scalar field φ.

The self-interactions of φ are described by the potential energy $V(\varphi^\dagger\varphi)$ [see equation (7)]. Depending on the values for μ^2, λ_3, and λ_6, V can have either one, two, or three minima. The discussion of the $V(\varphi^\dagger\varphi)$ extrema is relatively straightforward and will not be reproduced here. The relation between potential parameters and number of extrema is summarized in Table II.

The mass gap for the scalar excitations; that is, the mass associated with the complex scalar field, can be computed from (7) by writing $\varphi = v + \Phi$, where $v = \langle\varphi\rangle$ is the vacuum expectation value of φ and is assumed to be real. If φ can be rotated in such a way that it becomes a real field, then it follows that the quadratic term in $V(\Phi^2)$ is given by

TABLE II. The number of extrema of $V(\Phi)$ as a function of the potential parameters. Our definition for δ is $\delta = \lambda_4^2 - 4\mu^2\lambda_6$.

Item				
μ^2	λ_4	λ_6	δ	# Extrema
<0	>0	<0	0	1 Maximum
>0	<0	>0	0	1 Minimum
>0	>0	>0	>0	1 Minimum
>0	<0	>0	>0	5 Extrema
<0	any	>0	>0	3 Extrema

$$\tfrac{1}{2}M_\Phi^2\Phi^2 = 2v^2(\lambda_4 + 2v^2\lambda_6)\Phi^2, \tag{14}$$

and one can define the mass gap for scalar excitations as

$$\Delta_\Phi = M_\Phi = 2|v|\sqrt{\lambda_4 + 2v^2\lambda_6}. \tag{15}$$

The scalar mass gap is, then, independent of the gauge symmetry.

A nonvanishing M_Φ requires either a nonvanishing expectation value for $\langle\varphi\rangle$ or $\langle\varphi\rangle = 0$ and $\mu^2 > 0$. Furthermore, a nonvanishing scalar gap requires also that $\lambda_4 + 2v^2\lambda_6 > 0$, if $\langle\varphi\rangle \neq 0$.

From equations (14) and (15) it follows that the model is compatible with a nonvanishing φ vacuum expectation value (i.e., $\langle\varphi\rangle \neq 0$), in combination with a vanishing scalar gap if and only if $\lambda_4 = -2v^2\lambda_6$. In this case, the theory predicts a fermionic mass gap proportional to $\langle\varphi\rangle$, with no gap formation for the scalar excitations (i.e., the dispersion relation for the scalar excitations is linear in $|\vec{k}|$).

B. Fermionic mass gap

For the fermions fields, if φ and/or $\varphi^\dagger\varphi$ acquire a nonvanishing vacuum expectation value, then $\mathcal{L}$ acquires a mass term and a chiral mass term [see equations (4), (5), and (6)].

Let us assume that $\langle\varphi\rangle = v \neq 0$, with v being a real number. From the point of view of the fermions themselves, the interaction with the carbon structure shows up as

$$\widetilde{m}\overline{\psi}\psi + ih_2v^2\overline{\psi}\gamma_5\psi, \tag{16}$$

where $\widetilde{m} = 2g_1v + g_2v^2$. There is no reason *a priori* to require the positivity of $\widetilde{m}$ or h_2. Indeed, solving the free Dirac equation, with a mass term given by (16), gives the following dispersion relation:

$$\epsilon(\vec{p}^2) = \sqrt{\vec{p}^2 + \widetilde{m}^2 + h_2^2v^4}; \tag{17}$$

that is, the effective fermion mass is given by $\sqrt{\widetilde{m}^2 + h_2^2v^4}$ and the corresponding mass gap between valence and conducting bands is $2\sqrt{\widetilde{m}^2 + h_2^2v^4}$. The above reasoning is valid even when $\langle\varphi\rangle = 0$ and $\langle\varphi^\dagger\varphi\rangle \neq 0$. In this case $\widetilde{m} = g_2\langle\varphi^\dagger\varphi\rangle$ and $h_2\langle\varphi^\dagger\varphi\rangle$ replaces h_2v^2.

The coupling of the complex scalar field φ to the fermion degrees of freedom is given by

$$[g_1(\varphi+\varphi^\dagger)+g_2\varphi^\dagger\varphi]\overline{\psi}\psi+[h_1(\varphi-\varphi^\dagger)+ih_2\varphi^\dagger\varphi]\overline{\psi}\gamma_5\psi, \tag{18}$$

which has exactly the same structure as the mass term given by equation (16). Therefore, the status of the field φ can be translated into a dynamic fermion mass (i.e., a dynamic mass gap), which is both time- and space-dependent. The model accommodates graphene states where, for certain space-time regions, the system is gapless (i.e $\varphi \neq 0$) and others where $\varphi = 0$ and there is no gap. We are currently exploring the implications of this dynamic gap for graphene properties and will report the results elsewhere.

In graphene the fermionic mass gap Δ is a function of gauge symmetry. It follows that

$$U_A(1) \quad \Delta = 4|g_1 v|, \tag{19}$$

$$U_f(1) \quad \Delta = 2\sqrt{\tilde{m}^2+h_2^2v^4}, \tag{20}$$

$$U_b(1),\ U_f(1)\otimes U_b(1) \quad \Delta = 2\sqrt{g_2^2+h_2^2}v^2, \tag{21}$$

where Δ is twice the fermion mass.

C. Vector mass gap

It remains to discuss the mass gap for the vector excitations in graphene. The mass term for A_μ is generated by the scalar kinetic part of $\mathcal{L}$ [i.e., by $(D_\mu\varphi)^\dagger D^\mu\varphi$]. Therefore, unless the gauge transformation changes φ, the gauge field remains massless. It follows that

$$U_A(1) \quad \Delta_A = \sqrt{2}|g_1 v|, \tag{22}$$

$$U_f(1) \quad \Delta_A = 0, \tag{23}$$

$$U_b(1),\ U_f(1)\otimes U_b(1) \quad \Delta_A = \sqrt{2}|g_\varphi v|, \tag{24}$$

where Δ_A is the vector mass (i.e., the vector mass gap).

D. Gauge symmetries and gap relations

The mass (i.e., the gaps) for each of the fields in the model are generated via the Higgs mechanism. Besides the mass, the Higgs mechanism also provides a relation, dependent on the symmetry group, between the different gaps—see Table III for a summary of the results discussed in the previous sections.

A $U_A(1)$ chiral gauge theory implies a linear relation between the vector and fermion mass gaps $\Delta_A = \Delta/\sqrt{8}$, while $U_b(1)$ or $U_f(1)\otimes U_b(1)$ relate the two mass gaps by a quadratic equation $\Delta_A^2 = \Delta g_\varphi^2/\sqrt{g_2^2+h_2^2}$. For the gauge theory associated with the $U_f(1)$ symmetry, there is a mass gap for the fermionic and scalar degrees of freedom, but no gap for the vector excitations.

TABLE III. Mass gaps as a function of the gauge symmetry. See text for discussion. The scalar mass gap is independent of gauge group and for a nonvanishing vacuum expectation value if given by $\Delta_\Phi = 2|v|\sqrt{\lambda_4+2v^2\lambda_6}$.

Symmetry	Δ	Δ_A
$U_A(1)$	$4\|g_1 v\|$	$\sqrt{2}\|g_1 v\|$
$U_f(1)$	$2\sqrt{\tilde{m}+h_2^2v^4}$	0
$U_b(1)$	$2\sqrt{g_2^2+h_2^2}v^2$	$\sqrt{2}\|g_\varphi v\|$
$U_f(1)\otimes U_b(1)$	$2\sqrt{g_2^2+h_2^2}v^2$	$\sqrt{2}\|g_\varphi v\|$

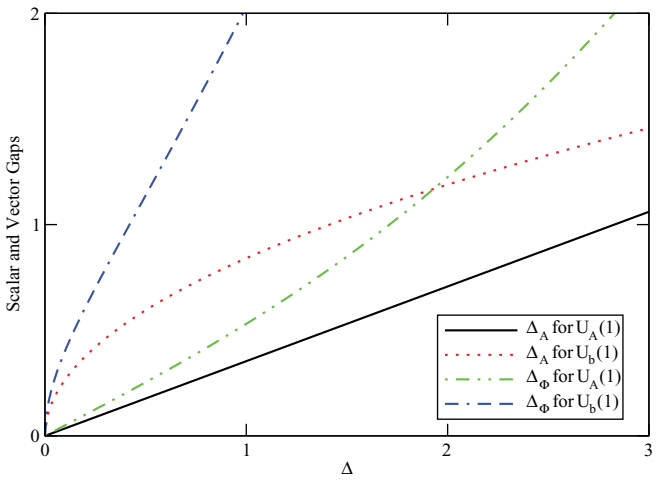

FIG. 1. (Color online) Δ_A and Δ_Φ as function of the fermionic mass gap Δ. The curves were computed setting all the coupling constants and the potential parameters to one and using arbitrary units.

A nonvanishing fermionic mass gap requires $\langle\varphi\rangle \neq 0$ or $\langle\varphi^\dagger\varphi\rangle \neq 0$, which by itself implies a scalar mass gap in graphene. The connection between the scalar mass gap Δ_φ and the remaining gaps is slightly more complicated than the relation between Δ and Δ_A.

The scalar, fermion, and vector mass gaps are functions of the coupling constants and of the φ vacuum expectation value. The connection between the mass gaps and the fundamental parameters of the theory depend on which global symmetry is gauged, as summarized in Table III. Moreover, all the mass gaps can be written in terms of the fermionic gap Δ. Therefore, if one is able to build graphene with different mass gaps, for example changing its doping and/or distortion, one can test which of the symmetries discussed before applies to graphene, if any, simply by looking at how Δ_A and Δ_Φ change with Δ. As an illustration, in Fig. 1 we show Δ_A and Δ_Φ as a function of Δ when all the coupling constants are set to unity. The figure uses arbitrary units. Clearly, the functional behavior distinguishes between a chiral gauge theory and a $U_b(1)$ or $U_f(1)\otimes U_b(1)$ gauge symmetry. Having $\Delta_A = 0$ for all values of Δ clearly points toward a $U_f(1)$ gauge theory.

Of the gauge theories discussed here, the mass gap relations do not distinguish between the two symmetries $U_b(1)$ and $U_f(1)\otimes U_b(1)$ because they provide similar types of φ-A_μ interactions. However, if $U_b(1)$ does not couple the fermions directly to the vector excitations, the $U_f(1)\otimes U_b(1)$ gauge symmetry has such a direct coupling between electrons and gauge field. Of course, if the strength of this coupling is extremely small, then the two theories will give exactly the same predictions for graphene. However, if the coupling $\overline{\psi}\gamma^\mu\psi A_\mu$ is sizable enough, then the fermionic interaction with the vector excitations will give relevant contributions to the dynamics of graphene and the two symmetries will provide different physics for vector and fermion excitations.

In the models discussed above, the gap in graphene is generated via spontaneous symmetry breaking. This is not the only way of having massive particles in a theory. For example, as discussed in Ref. 25, a fermionic gap can also be generated via dynamic symmetry breaking.

IV. EQUATIONS OF MOTION, VORTICES, AND FLUX QUANTIZATION

The equations of motion associated with the various fields are derived from $\mathcal{L}$ in the usual way. For fermions, they are given by

$$i\gamma^{\mu}D_{\mu}\psi - P(\varphi)\psi - P_5(\varphi)\gamma_5\psi = 0, \tag{25}$$

where $D_{\mu} = \partial_{\mu} + igA_{\mu}$ is the covariant derivative and A_{μ} is the gauge field. The corresponding equation for φ is

$$\begin{aligned} D^{\mu}D_{\mu}\varphi = &-(g_1 + g_2\varphi)\overline{\psi}\psi + (h_1 - ih_2\varphi)\overline{\psi}\gamma_5\psi \\ &- \mu^2\varphi - \lambda_4(\varphi^{\dagger}\varphi)\varphi - \lambda_6(\varphi^{\dagger}\varphi)^2\varphi, \end{aligned} \tag{26}$$

with the covariant derivative given by $D_{\mu} = \partial_{\mu} + ig_{\varphi}A_{\mu}$. The gauge field equation of motion reads

$$\partial_{\mu}F^{\nu\mu} = -g\overline{\psi}\gamma^{\nu}\psi - ig_{\varphi}\varphi^{\dagger}(D^{\nu}\varphi) + ig_{\varphi}(D^{\nu}\varphi)^{\dagger}\varphi. \tag{27}$$

Equations (25), (26), and (27) are the equations of motion derived from $\mathcal{L}$ taking into account all the possible coupling constants. In order to study each of the gauge theories considered previously, one has to take into account the corresponding constraints associated with the gauge group and summarized in Table I.

A. Vortex solutions

Let us now discuss vortex-like solutions for the bosonic sector of the theory, disregarding the coupling to the fermionic degrees of freedom. This provides a consistent solution for the field equations for the Dirac zero modes discussed in the next section.

In this section we will consider static solutions for equations (26) and (27) with

$$\varphi(\vec{r}) = \varphi_0(r)e^{in\theta}, \tag{28}$$

and

$$A^0 = 0, \quad A^i = \epsilon^{ij}\partial_j a = \epsilon^{ij}\frac{x_j}{r}a'(r), \tag{29}$$

where

$$a'(r) = \frac{da(r)}{dr} = b(r). \tag{30}$$

The equation of motion for φ then becomes

$$\frac{1}{r}\frac{d}{dr}\left[r\frac{d\varphi_0}{dr}\right] - \left(\frac{n}{r} + g_{\varphi}b\right)^2\varphi_0 = \mu^2\varphi_0 + \lambda_4\varphi_0^3 + \lambda_6\varphi_0^5, \tag{31}$$

and the gauge field equation simplifies to

$$\frac{1}{r}\frac{d}{dr}\left[r\frac{db}{dr}\right] - \frac{b}{r^2} = 2g_{\varphi}\left(\frac{n}{r} + g_{\varphi}b\right)\varphi_0^2. \tag{32}$$

Note that, only for the $U_A(1)$, $U_b(1)$, and $U_f(1)\otimes U_b(1)$ gauge theories (i.e., when $g_{\varphi} \neq 0$) are the scalar and gauge fields coupled. In this section we will consider only the $U_b(1)$ and $U_f(1)\otimes U_b(1)$ symmetries.

Let us first discuss the solutions of equations (31) and (32) at small distances. For $r \ll 1$, the gauge field equation becomes

$$\frac{1}{r}\frac{d}{dr}\left[r\frac{db}{dr}\right] - \frac{b}{r^2} = 0, \tag{33}$$

provided that $\varphi_0(r)$ is regular at the origin. The solution is

$$b(r) = b_1 r + \frac{b_{-1}}{r}, \tag{34}$$

where b_1 and b_{-1} are constants of integration. If $b_{-1} = 0$, equation (31) becomes

$$\frac{1}{r}\frac{d}{dr}\left[r\frac{d\varphi_0}{dr}\right] - \frac{n^2}{r^2}\varphi_0 = 0, \tag{35}$$

and its power-law solution reads

$$\varphi_0(r) = r^{|n|}. \tag{36}$$

On the other hand, if $b_1 = 0$ in (35), n^2 should be replaced by $(n + g_{\varphi}b_{-1})^2$ and the corresponding scalar-field solution at small r is

$$\varphi_0(r) = r^{|n+g_{\varphi}b_{-1}|}. \tag{37}$$

It follows that $\varphi_0(r)$ is always regular at the origin.

At large distances, for finite-energy solutions, φ approaches a constant value, a minimum of $V(\varphi_0^2)$, and the left-hand side of equation (31) vanishes. If $\varphi_0 \neq 0$, then

$$b(r) = -\frac{n}{g_{\varphi}r}, \tag{38}$$

and $b(r)$ is also a solution of equation (32). Note that this solution can be extended to the full range of r values, with the exception of the origin where a delta function sets in, coming from the Laplacian of b. On the other hand, if $\varphi_0 = 0$ (i.e., for pure graphene), one still has a solution for b as in (34). However, the requirement of finite energy demands $b_1 = 0$.

The vortex solutions include, as a particular case, the type of configurations considered in Ref. 19, where $b(r)$ is regular and $\varphi_0(r) \sim r^{|n|}$ for $r \ll 1$ and, for large r, φ_0 becomes constant and $b(r) \sim 1/r$. A class of vortices whose short-distance behavior is given by (37) was found. Furthermore, the zero modes of the Dirac equation computed in the next section require a vortex solution with φ_0 constant and nonvanishing and $b(r) = a'(r)$ given by (38) over all space, with the exception of the origin, as discussed previously. From the point of view of the gauge models, the singular behavior at $r = 0$ does not raise any conceptual problems. Indeed, we are using a continuous model to describe graphene and the dimensions of the unit cell provide a natural short-distance cutoff below which the model is no longer valid or, at best, should be corrected to take into account the crystal structure of the carbons and lattice defects.

If one takes the usual definition for the "magnetic field," $\vec{B} = \nabla \times \vec{A}$, it follows that $\vec{B}$ vanishes at large r. Close to the origin, $\vec{B}$ approaches a constant for a solution of the type of

(36) and vanishes for configurations such as (37). For both types of configurations, the vortex energy

$$\int d^2x \left\{ \frac{1}{2} B^2 + \left| \vec{D}\varphi \right|^2 + V(\varphi^\dagger \varphi) \right\} \tag{39}$$

is finite.

Despite the vanishing of $\vec{B}$ at large distance, the "magnetic flux" of the vortex configuration (29) over a sufficiently large-radius closed surface is quantized. Indeed, for a spherical surface centered at the origin,

$$\Phi = \int \vec{B} \cdot \vec{dS} = \int \vec{A} \cdot \vec{dl} = -2\pi r b(r) = \frac{2n\pi}{g_\varphi}, \tag{40}$$

where $n = 0, \pm 1, \ldots$ is the component of the angular momentum on an axis perpendicular to the graphene plan associated with the complex scalar field φ. Flux quantization opens the possibility of having Bohm–Aharonov-type effects in graphene without external electromagnetic fields, where electrons are scattered by a vector potential, which can be associated with a "topological defect" on the carbon structure, and acquire an extra phase. We call the reader's attention to the Bohm-Aharonov phases that have been observed in suspended graphene in association with mesoscopic deformations, where the measured charge-carrier mobility is substantially larger than in graphene on a substrate (see Ref. 26 and references therein).

V. FRACTIONALIZATION, DIRAC EQUATION, AND ZERO MODES

As discussed at the beginning of the present work, electron fractionalization is related to the normalizable zero modes of the Dirac kernel. The presence of these zero modes opens the possibility of observation of the fractional quantum Hall effect in graphene. A nice discussion connecting the Dirac equation zero modes with electron fractionalization can be found, for example, in Ref. 18.

For the $U_A(1)$ gauge theory, the proof of the presence of normalizable zero modes can be found in Ref. 19. The $U_f(1)$ gauge theory includes, as a particular case, the Dirac equation discussed by Hou, Chamon, and Mudry in Ref. 18. Therefore, for $U_f(1)$ gauge theory, fractionalization is possible. It remains to discuss the $U_b(1)$ and $U_f(1) \otimes U_b(1)$ gauge theories. In the following, it will be assumed that the bosonic sector is in a static vortex configuration with $A^0 = 0$,

$$A^i = \epsilon^{ij} \partial_j a(r), \quad \text{and } \varphi(\vec{r}) = \varphi_0(r) e^{in\theta}. \tag{41}$$

For a general gauge field, the Dirac equation associated with the $U_b(1)$ and $U_f(1) \otimes U_b(1)$ gauge theories is given by

$$\{-i\vec{\alpha} \cdot (\nabla - ig\vec{A}) + g_2(\varphi^\dagger \varphi)\beta + ih_2(\varphi^\dagger \varphi)\beta\gamma_5\}\psi = E\psi. \tag{42}$$

Let us define the following function:

$$\Delta(\vec{r}) = z\varphi_0^2(r) e^{i\alpha}, z = \sqrt{g_2^2 + h_2^2}, \tag{43}$$

where

$$\tan\alpha = -\frac{h_2}{g_2}. \tag{44}$$

With the above definitions and for the Dirac spinor

$$\psi = \begin{pmatrix} \Psi_+^b \\ \Psi_+^a \\ \Psi_-^a \\ \Psi_-^b \end{pmatrix}, \tag{45}$$

the Dirac equation becomes

$$\begin{aligned}
e^{-i\theta}\left(-i\partial_r - \frac{\partial_\theta}{r} - iga' \right)\Psi_+^a + \Delta(\vec{r})\Psi_-^a &= E\Psi_+^b, \\
-e^{i\theta}\left(-i\partial_r + \frac{\partial_\theta}{r} + iga' \right)\Psi_-^a + \Delta^*(\vec{r})\Psi_+^a &= E\Psi_-^b, \\
e^{i\theta}\left(-i\partial_r + \frac{\partial_\theta}{r} + iga' \right)\Psi_+^b + \Delta(\vec{r})\Psi_-^b &= E\Psi_+^a, \\
-e^{-i\theta}\left(-i\partial_r - \frac{\partial_\theta}{r} - iga' \right)\Psi_-^b + \Delta^*(\vec{r})\Psi_+^b &= E\Psi_-^a,
\end{aligned} \tag{46}$$

where a' means the derivative with respect to r of the function $a(r)$. These equations are invariant under the interchange of the two sublattices $a \leftrightarrow b$ provided that $\theta \to -\theta$ and $a' \to -a'$. This symmetry generalizes the sublattice symmetry of the Dirac equation already discussed in Ref. 18. We proceed by assuming that $\Psi_\pm^b = 0$. Note that, for zero modes, given a solution of the Dirac equation in sublattice a, the generalized sublattice symmetry generates another zero mode but leaving in sublattice b, or vice versa. If one writes

$$\begin{aligned}
\Psi_+^a &= \phi_+(r) e^{i(m\theta + \beta_+)}, \\
\Psi_-^a &= \phi_-(r) e^{i(k\theta + \beta_-)},
\end{aligned} \tag{47}$$

the zero-mode equations become

$$\phi_+' + \left(\frac{m}{r} + ga' \right)\phi_+ + z\varphi_0^2(r)\phi_- = 0, \tag{48}$$

$$\phi_-' - \left(\frac{k}{r} + ga' \right)\phi_- + z\varphi_0^2(r)\phi_+ = 0, \tag{49}$$

if the relations

$$k = m - 1 \text{ and } \beta_+ = \frac{\pi}{2} + \alpha + \beta_- \tag{50}$$

are satisfied. From equation (48) one can write

$$\phi_- = -\frac{1}{\Delta_0(r)}\left[\phi_+' + \left(\frac{m}{r} + ga' \right)\phi_+ \right], \tag{51}$$

where $\Delta_0(r) = z\varphi_0^2(r)$. Replacing this expression for ϕ_- in equation (49) one arrives at the following second-order differential equation:

$$\begin{aligned}
\phi_+'' + \left[\frac{1}{r} - \frac{\Delta_0'}{\Delta_0} \right]\phi_+' + \left[ga'' - \left(\frac{m}{r} + ga' \right) \right. \\
\left. \times \left(\frac{k}{r} + ga' + \frac{\Delta_0'}{\Delta_0} \right) - \frac{m}{r^2} - \Delta_0^2 \right]\phi_+ = 0.
\end{aligned} \tag{52}$$

The computation of a solution of equation (52) requires the knowledge of $\varphi_0(r)$ and $a'(r)$. Let us look for configurations where $\varphi_0(r)$ is a nonvanishing constant [i.e., a minimum of

$V(\varphi_0^2)]$. Then, $\Delta_0' = 0$ and $\Delta_0 = z\varphi_0^2$ is also a nonvanishing constant. The equation of motion of the scalar field (31) gives

$$b(r) = a'(r) = -\frac{n}{g_\varphi r}. \tag{53}$$

This particular gauge configuration solves the equation of motion for the gauge field (32), except at the origin where a Dirac delta function sets is due to the Laplacian operator. Our vortex solution requires a short-distance cutoff, which is provided by the dimensions of the graphene unit cell or the length scale associated with a defect. Indeed, for distances smaller than the unit-cell dimensions, the continuum description of graphene should break down.

For these vortex solutions, the gauge field is linked with the angular momenta, relative to an axis perpendicular to the graphene sheet, of φ. Furthermore, recall that the "magnetic field" associated with this type of vortex solution vanishes and, therefore, the energy associated with the vortex also vanishes.

For a vortex with a constant φ_0, equation (52) simplifies to

$$\phi_+'' + \frac{1}{r}\phi_+' + \left[-\frac{1}{r^2}\left(m - \frac{g}{g_\varphi}n\right)^2 - \Delta_0^2\right]\phi_+ = 0. \tag{54}$$

The solutions of this equation are the modified Bessel functions I and K of argument $\Delta_0 r$ for particular combinations of angular momenta associated with φ, ϕ_+, and ϕ_- (see Appendix A for details).

The gauge model has, at least, one normalizable zero-mode state of the Dirac equation. Therefore, the $U_b(1)$ and $U_f(1) \otimes U_b(1)$ gauge models can accommodate electron fractionalization without the presence of external electromagnetic fields. What is more, given the vortex solution and relation (53), besides fractionalization, the gauge models also incorporates flux quantization associated with the "magnetic field." The phase shifts coming from the Bohm-Aharonov effect associated with the vortex are connected with the component of the angular momenta of φ along an axis perpendicular to the graphene layer.

A. Zero modes and conformal invariance breakdown

The Sturm-Liouville form of the zero-mode equation is found by setting $\phi_+ = F/\sqrt{z}$ with $z = \Delta_0\, r$ in equation (54), which becomes

$$F'' + \frac{1}{z^2}\left[\frac{1}{4} - \nu^2\right]F = F, \tag{55}$$

where $\nu^2 = (m - \frac{g}{g_\varphi}n)^2$. This equation is equivalent to a one-dimensional Schrödinger eigenvalue problem with a potential $1/z^2$ which expresses invariance under scale change. The conformal symmetry is broken by the ultraviolet physics associated with defects or unit cell scales. Given that $\nu^2 \geqslant 0$, the potential strength for the Schrödinger problem is above the Breitenlohner-Freedman bound[35] and the corresponding quantum mechanical model is free from instabilities (i.e., the zero-mode state does not collapse). In other contexts (for example, in ultracold atomic physics), the violation of this bound gives rise to the Efimov effect.[36]

We observe the connection between the fermionic Sturm-Liouville equation and the dynamics of fermion fields in a supergravity anti-de-Sitter (AdS) background (see, for example, Ref. 37). In this description, the metric embodies conformal invariance leading to a $1/r^2$ potential associated, in our case, with the vortex solutions. The mass term of the fermionic field in the corresponding supergravity action contains the factor ν^2 (see, e.g., Ref. 38). Within this framework, the required short-range regularization (see the appendix) could be performed at the expense of introducing a dilaton field coupled to gravity, deforming the AdS metric.[39,40] This suggests that the Maldacena conjecture of the AdS-CFT (conformal field theory) duality[41,42] may well provide fresh insights to graphene physics. For example, the vector mass gap could be a consequence of breaking exact symmetries in holographic ten-dimensional backgrounds, encoding mass gaps for the fermionic field and vector fluctuations.[43]

VI. RESULTS AND CONCLUSIONS

In this paper we discuss gauge theories for graphene. The building of the gauge models starts by assuming that graphene dynamics can be described by fermion fields together with a complex scalar field φ. The field φ resumes the self-interaction of the carbon background and the mean fermionic self-interaction. After exploring the global symmetry of the most general Lagrangian, excluding derivative-like couplings, the corresponding gauge models are investigated.

The gauge models are compatible with a gap for fermion, vector, and scalar fields. The mass gaps are generated via a Higgs mechanism. Furthermore, the mass gaps associated with each gauge model are connected in different ways, which opens for the possibility of experimentally distinguishing between the models. Indeed, as claimed in Sec. III D for example, by changing the concentration of impurities in graphene, one can change the fermionic gap and check how the scalar and vector gaps adjust and, in this way, check which of the gauge models, if any, reproduce the graphene results. Furthermore, in what concerns the fermionic gap, within the models considered here, the mass gap is a dynamic quantity associated with the field φ.

The gauge models have finite-energy vortex solutions. Therefore, phenomena like the flux quantization of the "magnetic field," in association with topological defects of the carbon structure, and/or Bohm–Aharonov-type effects become possible within the description of graphene by gauge models. Several types of vortex solutions were discussed and, in general, the gauge field is linked with components of the angular momenta, along an axis perpendicular to the graphene plane, of φ. For this type of solution the phases associated with Bohm–Aharonov-type effects are a measure of the φ angular momenta.

Finally, we have investigated the two-dimensional Dirac equation for the vortex solutions. A generalization of the sublattice symmetry was discussed and we showed that all gauge models have normalizable zero modes together with a nonvanishing fermionic gap. Fractionalization is then possible in all the gauge models considered here. Within this theoretical background one expects that the fractional quantum Hall effect can take place in graphene in connection with the zero-mode solutions, even when there are no external electromagnetic fields. See also the discussion at the end of Sec. I.

The models investigated are potentially useful to describe graphene. Indeed, they unify, under the same dynamic principle, several features of graphene and predict others. The models have multiple parameters whose values should be found by reproducing experimentally known graphene properties. We are currently engaged in performing such an investigation and will report the results elsewhere.

ACKNOWLEDGMENTS

The authors acknowledge financial support from the Brazilian agencies FAPESP (Fundação de Amparo à Pesquisa do Estado de São Paulo) and CNPq (Conselho Nacional de Desenvolvimento Científico e Tecnológico).

APPENDIX : ZERO MODES OF THE DIRAC EQUATION

Let us discuss the solutions of equation (54), reproduced here:

$$\phi_+'' + \frac{1}{r}\phi_+' + \left[-\frac{1}{r^2}\left(m - \frac{g}{g_\varphi}n\right)^2 - \Delta_0^2\right]\phi_+ = 0. \quad \text{(A1)}$$

Introducing the adimensional distance $z = \Delta_0 r$, after multiplying this equation by z^2 one gets the following differential equation:

$$z^2\phi_+'' + z\phi_+' - \left[\left(m - \frac{g}{g_\varphi}n\right)^2 + 1\right]\phi_+ = 0, \quad \text{(A2)}$$

whose solutions are the modified Bessel functions $I_{\pm\nu}(z)$ and $K_\nu(z)$ (see Ref. 44 for definitions), where

$$\nu^2 = \left(m - \frac{g}{g_\varphi}n\right)^2. \quad \text{(A3)}$$

Note that ν can be a real number. Between $I_{\pm\nu}(z)$ and $K_\nu(z)$, only the latter tends to zero as $r \to +\infty$. Indeed, in this limit

$$K_\nu(z) = \sqrt{\frac{\pi}{2z}}e^{-z}, \quad \text{(A4)}$$

with its first derivative having a similar functional behavior. Therefore, modulo the behavior for small r, in principle, setting ϕ_+ proportional to K_ν the differential equation (54) is solved and the spinor is normalizable.

For small r

$$K_\nu(z) = \tfrac{1}{2}\Gamma(\nu)(\tfrac{1}{2}z)^{-\nu}, \quad \text{(A5)}$$

and the spinor diverges.

The divergence of ϕ_+ can be resolved as described in Ref. 45 in connection with the potential $-\beta/r^2$ with $\beta > 0$. A short-distance cutoff r_0 is introduced and the "potential" is replaced by its value at r_0. However, if ϕ_+ can be made regular at the origin, ϕ_- as given by (51) will diverge near the origin. Due to this short-distance divergence, ϕ_- is not normalizable unless the model has a minimal distance beyond which the continuum description of graphene no longer makes sense. The dimensions of the unit cell provide such an infrared cutoff. Remember that, in graphene, the carbon atoms are separated by $a \approx 1.42$ Å, and for $r < a$ one can set $\phi_\pm(r) \approx \phi_\pm(a)$ and have a continuous and normalizable spinor.

We call the reader's attention to the introduction of a short-distance (i.e., ultraviolet) cutoff for the fermion fields that does not change the results of Sec. IV A. Indeed, the Dirac zero modes give no contribution to the equations of motion associated with the vortex solution of Sec. IV A. In this sense, the flux quantization of the gauge field and the Bohm-Aharonov effect discussed there (i.e., the topological properties of the vortex solution), are independent of the Dirac spinors. On the other hand, the requirement that the Dirac spinors are normalizable is a necessary condition to have electron fractionalization (see, for example, the discussion in the work of Hou *et al.*[18]).

The singular behavior at $r = 0$ seems to be an indication of a "hole" at the center of the unit cell. This "hole" is a topological obstruction and is at the origin of the topological properties of the model analyzed in the present work.

[1] P. R. Wallace, Phys. Rev. **71**, 622 (1947).

[2] K. S. Novoselov, A. K. Geim, S. V. Morozov, D. Jiang, Y. Zhang, S. V. Dubonos, I. V. Gregorieva, and A. A. Firsov, Science **306**, 666 (2004).

[3] D. S. L. Abergel, A. Russell, and V. I. Falko, Appl. Phys. Lett. **91**, 063125 (2007).

[4] P. Blake, K. S. Novoselov, A. H. Castro Neto, D. Jiang, R. Yang, T. J. Booth, A. K. Geim, and E. W. Hill, Appl. Phys. Lett. **91**, 063124 (2007).

[5] C. Casiraghi, A. Hartschuh, E. Lidorikis, H. Qian, H. Harutyunyan, T. Gokus, K. S. Novoselov, and A. C. Ferrari, Nano Lett. **7**, 2711 (2007).

[6] A. H. Castro Neto, F. Guinea, N. M. R. Peres, K. S. Novoselov, and A. K. Geim, Rev. Mod. Phys. **81**, 109 (2009).

[7] N. M. R. Peres, Rev. Mod. Phys. **82**, 2673 (2010).

[8] K. S. Novoselov, A. K. Geim, S. V. Morozov, D. Jiang, M. I. Katsnelson, I. V. Grigorieva, S. V. Dubonos, and A. A. Firsov, Nature (London) **438**, 197 (2005).

[9] K. S. Novoselov, A. K. Geim, S. V. Morozov, D. Jiang, Y. Zhang, S. V. Dubonos, I. V. Grigorieva, and A. A. Firsov, Science **306**, 666 (2004).

[10] S. V. Morozov, K. S. Novoselov, F. Schedin, D. Jiang, A. A. Firsov, and A. K. Geim, Phys. Rev. B **72**, 201401 (2005).

[11] X. Du, I. Skachko, A. Barker, and Y. Andrei, Nature Nano. **3**, 491 (2008).

[12] Y. Zhang, Y.-W. Tan, Horst L. Stormer, and P. Kim, Nature (London) **438**, 201 (2005).

[13] V. P. Gusynin and S. G. Sharapov, Phys. Rev. Lett. **95**, 146801 (2005).

[14] N. M. R. Peres, F. Guinea, and A. H. Castro Neto, Ann. Phys. **321**, 1559 (2006).

[15] N. M. R. Peres, F. Guinea, and A. H. Castro Neto, Phys. Rev. B **73**, 125411 (2006).

[16] Y. Zhang, Z. Jiang, J. P. Small, M. S. Purewal, Y.-W. Tan, M. Fazlollahi, J. D. Chudow, J. A. Jaszczak, H. L. Stormer, and P. Kim, Phys. Rev. Lett. **96**, 136806 (2006).

[17] Y. Zhao, P. Cadden–Zimansky, Z. Jiang, and P. Kim, Phys. Rev. Lett. **104**, 066801 (2010).
[18] Y. Hou, C. Chamon, and C. Mudry, Phys. Rev. Lett. **98**, 186809 (2007).
[19] R. Jackiw and S.-Y. Pi, Phys. Rev. Lett. **98**, 266402 (2007).
[20] C. Chamon, C.-Y. Hou, R. Jackiw, C. Mudry, S.-Y. Pi, and G. Semenoff, Phys. Rev. B **77**, 235431 (2008).
[21] R. Jackiw and C. Rebbi, Phys. Rev. D **13**, 3398 (1976).
[22] W. P. Su, J. R. Schrieffer, and A. J. Heeger, Phys. Rev. Lett. **42**, 1698 (1979).
[23] R. Jackiw and J. R. Schrieffer, Nucl. Phys. B **190**, 253 (1981).
[24] C. E. Cordeiro, A. Delfino, and T. Frederico, Carbon **47**, 690 (2009); Phys. Rev. B **79**, 035417 (2009).
[25] A. J. Chaves, G. D. Lima, W. de Paula, C. E. Cordeiro, A. Delfino, T. Frederico, and O. Oliveira, e-print arXiv:1012.1374.
[26] M. A. H. Vozmediano, M. I. Katsnelson, and F. Guinea, Phys. Rep. **496**, 109 (2010).
[27] W. Ehrenberg and R. E. Siday, Proc. Phys. Soc. B **62**, 8 (1949).
[28] Y. Aharonov and D. Bohm, Phys. Rev. **115**, 485 (1959).
[29] Y. Aharonov and D. Bohm, Phys. Rev. **123**, 1511 (1961).
[30] F. D. M. Haldane, Phys. Rev. Lett. **61**, 2015 (1988).
[31] A. Hill, A. Sinner, and K. Ziegler, e-print arXiv:1007.0367.
[32] S.-S. Chern and J. Simons, An. Math. **99**, 48 (1974).
[33] S. Deser, R. Jackiw, and S. Templeton, Annals Phys. **140**, 372 (1982); Phys. Rev. Lett. **48**, 975 (1982).
[34] E. Witten, Commun. Math. Phys. **121**, 351 (1989).
[35] P. Breitenlohner and D. Z. Freedman, Ann. Phys. **144**, 249 (1982).
[36] E. Braaten and H.-W. Hammer, Phys. Rep. **428**, 259 (2006).
[37] O. Aharony, S. S. Gubser, J. M. Maldacena, H. Ooguri, and Y. Oz, Phys. Rep. **323**, 183 (2000).
[38] H. Forkel, T. Frederico, and M. Beyer, J. High Energy Phys. 07 (2007) 077.
[39] W. de Paula, T. Frederico, H. Forkel, and M. Beyer, Phys. Rev. D **79**, 075019 (2009).
[40] W. de Paula and T. Frederico, Phys. Lett. B **693**, 287 (2010); Int. J. Mod. Phys. D **19**, 1351 (2010).
[41] J. Maldacena, Adv. Theor. Math. Phys. **2**, 231 (1998).
[42] E. Witten, Adv. Theor. Math. Phys. **2**, 253 (1998).
[43] M. Bianchi and W. de Paula, J. High Energy Phys. 04 (2010) 113.
[44] M. Abramowitz, I. A. Stegun, *Handbook of Mathematical Functions* (Dover Publications Inc. New York).
[45] L. D. Landau and L. E. Lifshitz, *Quantum Mechanics* (Pergamon Press, 1977).